JACS
JOURNAL OF THE AMERICAN CHEMICAL SOCIETY
Article
pubs.acs.org/JACS

Model Calculations Suggest that the Central Carbon in the FeMo-Cofactor of Nitrogenase Becomes Protonated in the Process of Nitrogen Fixation

Per E. M. Siegbahn*

Department of Organic Chemistry, Arrhenius Laboratory, Stockholm University, SE-106 91, Stockholm, Sweden

Supporting Information

ABSTRACT: Nitrogen activation by nitrogenase is one of the most important enzymatic processes on earth. In spite of the determination of X-ray structures of increasingly higher resolution, the nitrogenase mechanism is still not understood. In the most recent X-ray structures it has been shown that a carbon resides in the center of the MoFe-cofactor. Its role is not known. Recent spectroscopic studies, mainly EPR, have come closest to obtaining a molecular mechanism for activating nitrogen. Two hydrides have been shown to play a key role in this context. In the present study, the mechanism for nitrogenase has been investigated by hybrid DFT using a cluster model. This approach has been shown to be very successful for predicting mechanisms for other redox-active enzymes, such as the one for photosystem II, but has so far not been used in its most recent form for nitrogenase. The mechanism obtained has large similarities to the one suggested by spectroscopy, with a reductive elimination of two hydrides just before nitrogen binding. However, a very surprising finding is that the central carbon becomes protonated and has to move out of the cavity as a methyl group before the hydrides can be formed. This has not been suggested before.

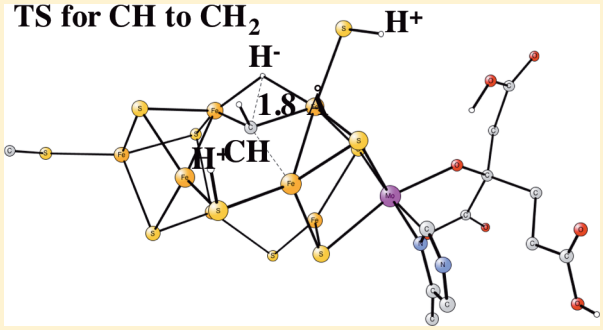

1. INTRODUCTION

During the past decade a large number of enzymatic redox reactions have been mapped energetically by model calculations,[1] most noteworthy water oxidation in photosynthesis.[2] Nitrogen fixation by nitrogenase is perhaps the most interesting one which has not yet been treated with the same general methodology. Even though substantial progress has been made experimentally, there are still major points remaining to be understood in the mechanism. In the present study, the steps leading up to nitrogen activation has been studied in detail, with emphasis on the energetics.

The reaction catalyzed by nitrogenase is $N_2 + 8(H^+, e^-) \rightarrow 2NH_3 + H_2$. Sixteen ATP are consumed in this process. An X-ray structure of the enzyme was obtained already in 1992,[3] showing that the active FeMo-cofactor is composed of one molybdenum and seven irons, bound together by sulfides into two connected cubanes. Ten years later, an X-ray structure at a very high resolution of 1.16 Å showed that there was a first row atom in the center of the cofactor, which was a major surprise.[4] Even higher resolution and a spectroscopic analysis were required to identify the atom as carbon.[5,6] Very recently, a high-resolution structure with a bound CO has also been reported.[7]

In the meantime, during the past decade, major advances were made in the understanding of the nitrogenase reaction using spectroscopic techniques. In 2005, a hydride intermediate was isolated and characterized.[8] The couplings indicated that there were two bridging hydrides. Cryoannealing revealed that this is the intermediate that has accumulated $4e^-/4H^+$ (the E_4 state).[9] In 2009, an N_2 intermediate was trapped,[10] recently identified as E_4 with two hydrides and two nitrogens.[11] In 2010, ^{95}Mo ENDOR of E_4 indicated that Mo is not one of the metal atoms that bind the hydrides.[12] This means that the Fe-part of the cofactor binds the two hydrides, probably in bridging positions. In 2011, ^{57}Fe ENDOR spectroscopy suggested that the FeMo-cofactor cycles through only one redox couple.[13] In 2013, it was concluded that there is a reductive elimination mechanism for H_2/N_2 binding.[14] Very recently, in 2015, it was shown that the reductive elimination/oxidative addition equilibrium is kinetically as well as thermodynamically reversible.[11] This reversibility proves that the equilibrium is very nearly iso-energetic. The present view on the mechanism for nitrogenase is summarized in a recent review.[15]

During the first decade after the first X-ray structure, mainly two theoretical groups, the groups of Noodleman[16] and Dance[17] were involved in mechanistic work. This work was, of course, quite hampered by the fact that the presence of the atom in the center of the cluster, atom X, was not known. Nevertheless, very detailed investigations of optimal redox states were made using advanced broken symmetry techniques. Without the atom X, Noodleman et al.,[16] using a variety of density functionals, concluded that the resting state should be $Mo^{4+}6Fe^{2+}1Fe^{3+}$, which produced metal hyperfine and

Received: April 26, 2016
Published: July 25, 2016

DOI: 10.1021/jacs.6b03846
J. Am. Chem. Soc. 2016, 138, 10485−10495

Mössbauer isomer shifts that agreed well with experimental results. Interestingly, the geometries were also in excellent agreement with experiments even without the X atom. A later study including X as a nitrogen gave the assignment $Mo^{4+}4Fe^{2+}3Fe^{3+}$. It was found difficult to conclude the identity of X based on comparisons to spectroscopic results.

Using DFT with the BLYP functional, Dance derived a chemical mechanism for ammonia formation.[17] An important part of the mechanism was that the protons are supplied via a chain of residues including water molecules that end at two specific sulfurs. A full diagram including transition states for 21 steps were calculated. N_2 was found to be η^2-coordinated to an endo position of one Fe atom of a prehydrogenated FeMo cofactor, where the reaction passes through N_2H_2 and N_2H_4 intermediates. Hydrogenation of N_2 and the intermediates were suggested to be intramolecular and not involving direct protonations from surrounding residues. The interstitial X atom was chosen as nitrogen.

Blöchl et al. studied N_2-binding to the FeMo-cofactor using Car−Perinello molecular dynamics with the PBE functional and found axial and bridging binding modes of N_2 to the prismane Fe-sites followed by cleavage of a protonated sulfur bridge.[18] The binding to molybdenum was found to be endergonic. Two different pathways for ammonia formation were found, one starting with a bridging N_2 and the other one an axially bound N_2. These pathways were found to connect at an early stage in the mechanism. Nørskov et al. studied the entire mechanism including N_2H_2 and N_2H_4 intermediates.[19] Protonations were found to occur in an alternating fashion on the two nitrogens with the initial reduction of N_2 being rate-limiting. In a much more recent study Nørskov et al. suggested that the cofactor needed an activation where H_2S was removed to bind N_2.[20] Huniar et al. studied several steps in the catalytic cycle using the BP86 and B3LYP functionals.[21] A nitrogen was used as X. They suggested that the central N atom was first fully protonated to NH_3, which then disappeared from the cluster. After this elimination, N_2 could bind in the cavity of the cluster with a $Mo^{4+}6Fe^{2+}1Fe^{3+}$ configuration. That mechanism was later discarded experimentally because in an ESEEM/ENDOR study an exchange of a central nitrogen atom could be excluded.[22] Recently Szilagyi et al., using the BP86 and B3LYP functionals, suggested a resting state, $Mo^{4+}2Fe^{2+}5Fe^{3+}$, which is more oxidized than earlier proposals.[23] A central carbon atom was used, and the homocitrate ligand was found hydroxyl-protonated. Even more recently, Yan et al.[24] performed a combined experimental (FTIR) and theoretical (DFT with PBE) study of CO bound to the FeMo-cofactor. The structures with the best match between measured and calculated frequencies were used to identify the binding positions.

The present investigation of the mechanism started out by a calculation of the energetics for adding electrons and protons to the FeMo-cofactor. It was found that the cofactor itself is quite negatively charged by −4. No other charge state gave reasonable energetics. The high negative charge is compensated by two positive arginines and one histidine that is sometimes protonated. The best results for the spin-coupling is an alternating state with as many antiferromagnetic couplings as possible. The oxidation state of Mo was found to be III as suggested based on spectroscopy.[25]

For readers not familiar with the present modeling, some comments could be useful. It may initially seem surprising that a model with only 200 atoms should give a reasonable picture of the mechanism of an enzyme, particularly for a redox active enzyme. However, it has been found in numerous applications on more than 30 enzymes that the chemistry occurring at the active site is quite local, well-described by the present modeling.[1] It is important to note that for the steps where electrons and protons enter the active site key experimental information has to be used because the small model does not describe the long-range effects well. For example, the exergonicity of the full catalytic cycle is explicitly used to define the absolute reference for adding an (e^-, H^+), as explained below. For these removals, long-range effects are furthermore minimal because the charge does not change. Among the enzymes very well described by the modeling, several important ones can be found, like photosystem II (PSII), cytochrome c oxidase, ribonucleotide reductase, methane monooxygenase, hydrogenase, and methyl coenzyme M reductase. In the case of PSII, detailed results were predicted, which only several years later became completely verified by experiments. The predictions made by analyzing experiments were in most cases much less successful. It can therefore no longer be argued that results predicted by this type of modeling are just speculative, at least certainly not more speculative than those obtained by analyzing experiments.

2. METHODS AND MODELS

The methods used here are essentially the same as the ones used for many other enzymes, summarized in a recent review.[1] The hybrid functional B3LYP*[33,34] was used with polarized basis sets for the geometries (lacvp*), large basis sets for energies, and a surrounding dielectric medium with a dielectric constant equal to 4.0 (basis lacvp*). The performance of the B3LYP functional for the present type of problems has been reviewed,[35−37] indicating a typical accuracy within 3−5 kcal/mol, normally overestimating barriers. Dispersion effects were added using the empirical D2 formula of Grimme.[38] A minor difference from earlier studies is that a different large basis set has been used, the 6-311+G(2d,2p) set. This change was forced by convergence problems but should have minimal effects on the energetics. Hessians were calculated for the evaluation of zero point effects and for determining transition states. Unlike earlier studies, entropy effects were also evaluated by projecting out the frozen coordinates from the Hessians. The calculations were performed with the programs Jaguar[39] and Gaussian09.[40]

The model of the FeMo-cofactor is based on the high-resolution structure[5] and is shown in Figure 1. The points fixed from the X-ray structure are marked with red stars. The sulfurs as well as the oxo-connections between molybdenum and homocitrate are unprotonated. The dangling carboxylates of the homocitrate were protonated to avoid artificial buildup of spin. The nearest amino acids, some of them found to be essential in catalysis, were included in the model. These are His442, Cys275, His195, Val70, Gln191, Glu380, Phe381, Arg96, and Arg359. In order to activate N_2 it was found that the charge state of the model should alternate between −1 and −2. Optimization of the structure for a −1 charge led to the surprising result that the cofactor itself became negative by as much as −4. Instead, both His195 and Glu380 (neutralized) became protonated, as well as Arg96 and Arg359.

A thorough investigation of the optimal spin states was initially performed. This led to essentially the same conclusions as in previous studies of the same system. The best spin-coupling is an alternating state with as many antiferromagnetic couplings as possible. Mo has a negative spin and Fe1 in the other end has positive spin. Fe2−Fe4 have negative and Fe5−Fe7 positive spins. The oxidation state of Mo for most structures studied here was found to be III (with spin-population 2.6−2.8) as also suggested based on spectroscopy.[25] A Mo(IV) oxidation state would by experience have a population around 2.0 for a triplet coupling and zero for a singlet coupling. It can be noted that for the structure shown in Figure 1 the spin-population is 2.3 indicating that there can be some mixture between Mo(III) and

DOI: 10.1021/jacs.6b03846
J. Am. Chem. Soc. 2016, 138, 10485−10495

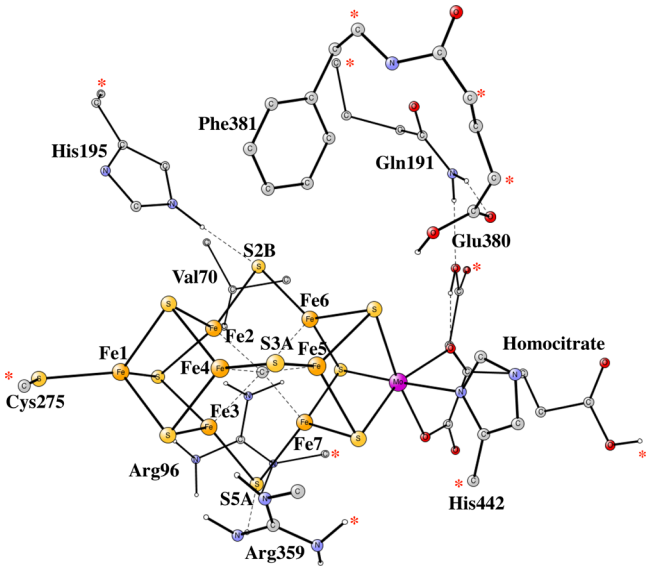

Figure 1. Model used for the studies of the nitrogenase mechanism. Most hydrogens are omitted. The numbering of the Fe atoms is the same as in the X-ray structure. Stars mark atoms fixed from the X-ray structure. The electronic structure is $Mo^{3+}5Fe^{2+}2Fe^{3+}$. This state is termed A_0^1 in the text.

Mo(IV). The spins on the irons are almost completely delocalized, with spin-populations normally between 3.5 and 3.7, making an assignment of oxidation states for the individual irons difficult. With a charge of −4 and assuming a charge of carbon of −4, a formal spin-assignment can then be written as $Mo^{3+}5Fe^{2+}2Fe^{3+}$. In the sequence of events discussed below, the even-electron systems are normally singlets, and the odd-electron systems are normally doublets. The few exceptions are mentioned explicitly.

A minor problem can be mentioned in this context, and this is that the resting state was also found to be a doublet although it should be a quartet.[14] The energy difference is 4.1 kcal/mol, which is a common error for spin-splittings in DFT calculations. When the proton on His195 is removed, the splitting goes down to zero, indicating a model problem with this residue; see further below. Therefore, absolute redox energies may have a somewhat larger error than other energies. From experience, it is known that relative redox energies have a higher accuracy.

The driving force for the entire reaction $N_2 + 8\ (H^+,e^-) \rightarrow 2\ NH_3 + H_2$ was taken from experiments to be 230 kcal/mol, using an estimated redox potential of the electron donor of −1.6 V under active conditions.[26−28] The electron donor is the so-called P-cluster, which is a nearby 8Fe−8S cluster. The redox potential of the P-cluster is −0.4 V, but the two ATP's consumed each have a decreasing effect of −0.6 V.[29] Ideally, this would mean that the present electron affinities should be compared to the value of 62 kcal/mol (4.281−1.6 V), and the proton affinities should be compared to 279.8 kcal/mol, corresponding to the energy of a proton in water. However, some adjustments to these values have been used, with 59.3 and 286.3 kcal/mol, respectively, which leads to a matching of the experimental driving force of 230 kcal/mol. A more important correction to the results was obtained from results obtained during the course of the present study. It was found that the computed pK_a of His195 became much too high. A closer look at the region surrounding this residue indeed showed important charge interactions, mostly from a nearby arginine, Arg277, which was left out of the model. Therefore, the calculated pK_a was shifted down by 5 pK_a units (7.0 kcal/mol). Ideally, the problem can instead be fixed by using a much larger model, and this will be attempted in the future. It should be added that this problem was not noticed until near the end of the present two year study. In the process of activating the cofactor (see below), it did not have any effect, but when N_2 binds, the shift of the pK_a of His195 is quite important. In summary, a value of 286.3 kcal/mol was subtracted from the calculated proton affinities, except for the protonation of His195, from which a value of 293.3 kcal/mol was subtracted. For the calculated electron affinities, a value of 59.3 kcal/mol was subtracted. The pK_a and the redox potentials obtained can then be compared to pK_a 7 for the proton donor and redox potential of the electron donor of −1.6 V, respectively, to obtain the energies in the diagrams.

An important fact coming out of the above energies is that formation of H_2 will be quite exergonic in nitrogenase. The combined cost of getting one proton from water and one electron from the P-cluster is (286.3 + 59.3) = 345.6 kcal/mol. The energy of H_2 of 1.175497 au is equal to 737.6 kcal/mol. Forming H_2 is therefore exergonic by 2 × 345.6 − 737.6 = −46.4 kcal/mol. It is clear that to prevent unnecessary H_2 formation there has to be strict kinetic control in all steps of the process.

3. RESULTS

The present investigation of the mechanism started out from the high-resolution structure of the FeMo-cofactor.[5] This structure has no protons on sulfur. A surprising initial finding was that the cofactor becomes charged by as much as −4, even though the chemical model used is charged by only −1. This is possible by having positively charged residues in the second sphere of the cofactor, two arginines and a protonated histidine. Also, a glutamate surprisingly takes a proton from the cofactor. A high negative charge of the cofactor is probably necessary for forcing incoming electrons from the electron donor to go to nitrogen during the catalytic cycle instead of going to the cofactor. In the investigation of the mechanism, electrons and protons were added, and the redox potentials and pK_a values were calculated. The results are shown in Table 1. A nomenclature is used which is in analogy with the one used for PSII.[2] This means using two indices, the lower one denoting the state defined by the number of electrons added and the upper one relating to the charge state of the complex. For every reduction step there are two charge states, the first one denoted by 1 for the charge state of the starting structure and the second one denoted by 0 for the state when an electron and no proton has been added. E_4^0 (or A_4^0 state, see below) therefore means the E_4 (or A_4) state with an electron but no proton added compared to the E_3^1 (or A_3^1) state. In the discussion below, the transfer of one (e^-, H^+) constitutes one step. Sometimes the proton has to move over several positions before the lowest energy is obtained. It should be noted that absolute redox potentials are sensitive to the chemical model used and are

Table 1. Redox and pK_a Values at the Different Stages of the FeMo-Cofactor Reduction[a]

state	protonation site	redox	pK_a
A_0^1			
A_1^0	S3A	−1.2	
A_1^1	S2B		16.1
A_2^0		−1.1	
A_2^1	His195		7.9
A_3^0	C	−1.2	
A_3^1	CH		7.4
A_4^0	CH	−1.3	
A_4^1	CH_2		13.4
A_5^0	CH_2	−1.2	

[a]The redox potential of the reference electron donor is −1.6 V. The starting A_0^1 state is shown in Figure 1.

DOI: 10.1021/jacs.6b03846
J. Am. Chem. Soc. 2016, 138, 10485−10495

therefore somewhat uncertain. Relative redox potentials are much more certain.[1]

The initial investigation was obviously concerned with identifying the structures with hydrides that have been observed experimentally. Very surprisingly, all hydride positions investigated have very poor energies compared to other protonation sites. This was found irrespective of how many electrons and protons that were added to the X-ray structure. There were three possibilities. First, there could be a very unusual error using the present methodology. This is very unlikely considering the quite high accuracy for the binding of hydrides that has been obtained previously for the similar case of hydrogenases.[41,42] The error in the calculations would have to be larger than 20 kcal/mol to allow hydride binding. A second explanation would be that the experimental assignment of the hydrides is not correct. This is also very unlikely. The EPR coupling constants measured are quite characteristic for hydrides. The third and remaining possibility is that the experimental X-ray structure in a significant way does not correspond to the structures with the hydrides that has been observed spectroscopically. Initially, this also appeared very unlikely, but this was the track that was continued in the subsequent investigations during the past two years.

3.1. FeMo-Cofactor Activation. The starting structure for the systematic investigation of redox and pK_a values is the structure shown in Figure 1, which has no protons on the sulfurs. This state will here be termed A_0^1. For this state, the first electron was found to enter with a redox potential of −1.2 V, leading to an exergonic transfer by −8.6 kcal/mol. The state formed is A_1^0. As the electron reaches the cofactor, the proton on His195 (initially protonated) goes over to the sulfur S2B between Fe2 and Fe6. After this, the unprotonated His195 forms only a weak hydrogen bond to the cofactor. In many steps, a similar scenario occurs after each electron transfer to the cofactor, keeping the charge of the cofactor itself constant at −4 during the reduction. The optimal position for the proton transferred from His195 is not on S2B but on the sulfur S3A between Fe4 and Fe5, so the proton has to move. This transfer does probably not occur over the cofactor but instead by a deprotonation of S2B to the surrounding medium followed by a protonation of S3A from the surrounding. The pK_a value is 16.1, leading to an exergonic proton transfer by −12.7 kcal/mol. The total energy gain of the first transfer of an (e^-, H^+), leading to state A_1^1, is thus −21.3 kcal/mol. S3A is now protonated.

The second electron has a redox potential of −1.1 V and an exergonic transfer to state A_2^0 by −11.2 kcal/mol, including a deprotonation of His195 to S2B. The second proton from the medium goes to the unprotonated His195. The protonation state of the cofactor actually has two choices, and this was a major surprise in the present study. The pK_a for the proton on S2B is almost identical to the one obtained by placing the proton on the central carbon. The pK_a values are 7.9 and 8.3, respectively. At this point, the calculations indicate that protonation of the carbon is kinetically hindered. The energy gain of the second transfer of an (e^-, H^+), leading to state A_2^1, is −12.5 kcal/mol. Both S2B and S3A are now protonated.

As the third electron enters, it is again favorable for a proton on the protonated His195 to go to the cofactor. Both S2B and S3A are now already protonated, so the proton will initially go to S5A. This leads to a rather low redox potential of −1.2 V and an exergonic transfer by −8.6 kcal/mol, leading to state A_3^0. At this point the proton on S5A can move with a low cost to a hydride position on Fe6 and after that to the central carbon with a total barrier of only 10.9 kcal/mol. This corresponds to a rate of 10^5 s^{-1}, and the process is almost thermoneutral. The optimal protonation state before the next proton from the medium is added is actually a doubly protonated carbon, but the second proton transfer to carbon is kinetically hindered at this stage. The next proton from the medium goes to the unprotonated His195. The sulfurs protonated are S2B and S3A; the other ones are unprotonated. The central carbon is a CH-state. The pK_a value for the added proton on carbon is 7.4 leading to an overall exergonic transfer by −8.7 kcal/mol of the third (e^-, H^+) going from state A_2^1 to state A_3^1. The energy cost for keeping carbon unprotonated is relatively low (1.7 kcal/mol at this stage, see later however).

One might argue that the protonation of His195 to reach an A_3^1 state is faster than the transfer of the proton to carbon in A_3^0 and might therefore hinder the protonation of the carbon. However, even if the proton is already on His195, the barrier for protonation of carbon in A_3^1 is relatively low, 13.9 kcal/mol, corresponding to a rate of 10^2 s^{-1}. This reaction is exergonic by −2.9 kcal/mol.

Several other structures were optimized for A_3^1. One of them was to protonate one of the oxygens on the homocitrate. In that case, the energy goes up by as much as 15.7 kcal/mol. Some of these results are general for all structures. For example, the two sulfurs most easily protonated are always S2B and S3A. To protonate S5A is always less favorable, which is due to the positive neighboring arginines, Arg96 and Arg359. The best one with a central CH_2 has only S3A protonated. Furthermore, many attempts were tried at several stages of the process to create an open site on molybdenum, but they all required high energies. This does not necessarily mean that these states with higher energies never enter the activation process or the catalytic cycle. They could still in principle appear as unstable intermediates.

The fourth electron starts with a central CH group, and as in most of the other cases, a proton now moves to the cofactor from His195. The initial protonated cofactor with the lowest energy was actually found for a hydride bridging between Fe2 and Fe6. This leads to a redox potential at this stage of −1.3 V and an exergonic transfer of the electron by −8.1 kcal/mol. From this point, the hydride can very easily move over to carbon and form a CH_2 group. The transfer barrier is only 3.4 kcal/mol, corresponding to a very high rate, and the transfer is exergonic by −7.3 kcal/mol. The redox potential including this proton transfer is −0.9 V leading to an exergonic transfer by −15.4 kcal/mol from state A_3^1 to state A_4^0. The next proton goes as usual to the unprotonated His195, with a pK_a of 13.4, which makes the protonation exergonic by −9.0 kcal/mol. Addition of the fourth (e^-, H^+) is therefore exergonic by −24.4 kcal/mol. At this point, the energy with a central unprotonated carbon instead is very unfavorable, + 20.9 kcal/mol higher than with a central CH_2 group.

In summary, A_0^1 has no protons on sulfur, A_1^1 has a proton on S3A, and A_2^1 has protons on both S2B and S3A. After that, the central carbon becomes protonated. A_3^1 has a CH group in the center, and A_4^1 has a CH_2 group in the center.

Even after the fourth reduction of the cofactor, there is no positive binding energy for N_2 to the cofactor. There is a small enthalpic binding in an end on position on Fe6, for example, but it is far away from overcoming the loss of entropy. For these structures N_2 is entirely unperturbed from the gas phase and has no spin. To obtain a state which binds and activates N_2,

DOI: 10.1021/jacs.6b03846
J. Am. Chem. Soc. 2016, 138, 10485−10495

still another electron is needed. When the electron arrives, the proton from His195 moves into a hydride position between Fe2 and Fe6 on the cofactor. The redox potential for this electron transfer step is −1.2 V, leading to an exergonic transfer by −9.5 kcal/mol. The hydride can then move over a barrier of 11.8 kcal/mol to the central CH_2 group to form CH_3. The best position for the methyl group found so far is terminally bound to Fe6, but a terminal position on Fe2 has almost the same energy. The redox potential, including the exergonic formation of CH_3 by −5.8 kcal/mol, is −0.9 V, leading to state A_S^0 (Figure 3). The full process of electron transfer is exergonic by −15.3 kcal/mol. For the resulting A_S^0 state, the electronic structure is $Mo^{3+}4Fe^{2+}3Fe^{1+}$.

For the A_S^0 state, the energy required for opening up the cavity is small, and N_2 can now bind as shown in Figure 4 and form a triplet state. The optimal singlet state, 1.1 kcal/mol above the triplet, is also shown for comparison. The rather open triplet state is best suited for the first protonation of N_2, but the singlet state is more activated with a larger spin on N_2. The enthalpic binding energy for N_2 in the open triplet state is 8.1 kcal/mol. The different contributions to this value are interesting. The binding energy without solvent, dispersion, zero-point, and entropy effects is strongly negative by −7.7 kcal/mol. The solvation effect increases the binding by +5.6 kcal/mol, and the dispersion effect is as large as +11.1 kcal/mol. The zero-point contribution is negative by −0.9 kcal/mol. The total enthalpic binding energy of +8.1 kcal/mol is not enough for compensating the loss of translational entropy for N_2 of −9.9 kcal/mol. However, there is one more positive effect of +5.7 kcal/mol coming from the change of entropy of the cofactor itself when it opens up to form the more loosely bound cluster. The net binding of N_2 is therefore +3.9 kcal/mol. From this point, electrons and protons can be added to N_2, as will be descibed in a future paper.

Starting from the X-ray structure in Figure 1, there are four exergonic (e^-, H^+) transfers from A_0^1 to A_4^1, with energies −21.3, −12.5, −8.7, and −24.4 kcal/mol, respectively, displayed in Figure 2. An exergonic electron transfer by −15.3 kcal/mol leads up to the structure shown in Figure 3, which binds N_2 with a binding free energy of 3.9 kcal/mol. The main problem with this mechanism of activating N_2 is that no hydrides have been formed, as strongly suggested by experiments. In fact, the best A_4^1 state (with a CH_2 group) is as much as 31.7 kcal/mol lower in energy than the best one with a central carbon and two hydrides. Therefore, another scenario is suggested here to explain the experimental observation of hydrides.

A puzzling fact in connection with the present results is that whenever the cofactor has been studied by spectroscopy even after the activation of N_2 there is an unprotonated carbon in the center. This means that there has to be a way for the cofactor to return to the original structure. The first step in this process could be going back in the activation process from the terminal CH_3 toward a CH_2 in the center and a bridging hydride. This step is endergonic by 5.8 kcal/mol (Figure 2). However, continuing the process by losing a hydrogen molecule going from A_S^0 to A_3^0 to form a CH group in the center is strongly exergonic, partly because of a large gain of translational entropy for the free H_2 molecule of 10.3 kcal/mol. In the final step to reach a cofactor with an unprotonated carbon in the center, going from A_3^0 to A_1^0, another hydrogen molecule is lost in a process which is also strongly exergonic. It is clear that these processes must be quite slow not to compete with the catalytic cycle and therefore must be regulated kinetically. However,

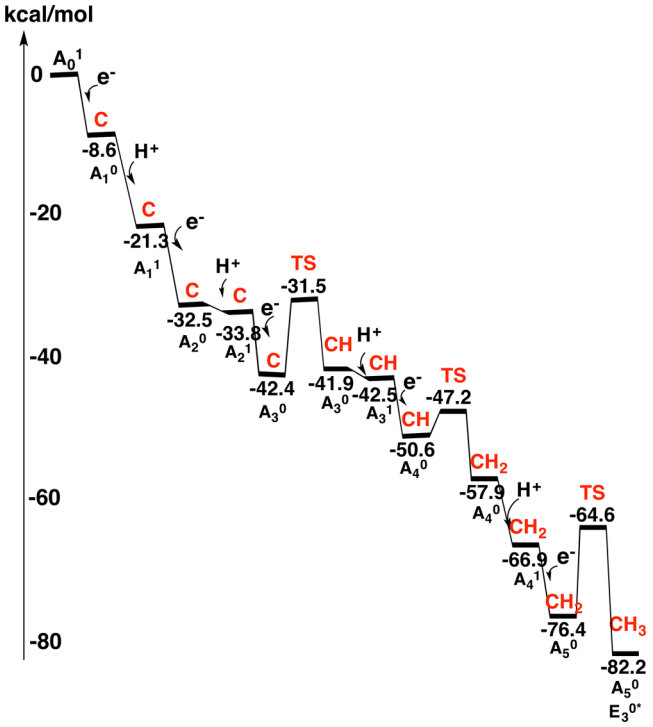

Figure 2. Energy diagram for the activation process of the FeMo-cofactor. The protonation state of the central carbon for each state is shown in red.

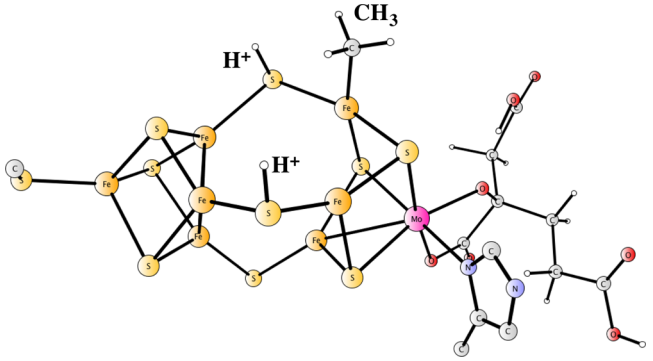

Figure 3. Core structure of the A_S^0 state (or E_3^0*) The electronic structure is $Mo^{3+}4Fe^{2+}3Fe^{1+}$. Surrounding residues and most hydrogen atoms are omitted.

when the ATP ceases, there is more time to go back to the central unprotonated carbon in the cofactor than during catalysis.

A problem in the present mechanistic scenario is to avoid a state where the methyl group takes a proton from the sulfur to form methane, which then would leave the cofactor. Even though this process is quite exergonic, it is considered unlikely since this would make it much more difficult for the cofactor to be restored to its original form after the catalytic cycles are finished. In fact, experiments speak strongly against this possibility. The X-ray structures all have a carbon atom in the center, and the procedure used for the enzyme in the initial incorporation of the carbon, requiring other enzymes,[43] is impossible under the conditions the X-ray structures are studied. The suggestion is therefore that formation of methane is kinetically hindered. For the structure in Figure 4, the barrier for formation of methane is indeed high with 21.1 kcal/mol,

DOI: 10.1021/jacs.6b03846
J. Am. Chem. Soc. 2016, 138, 10485−10495

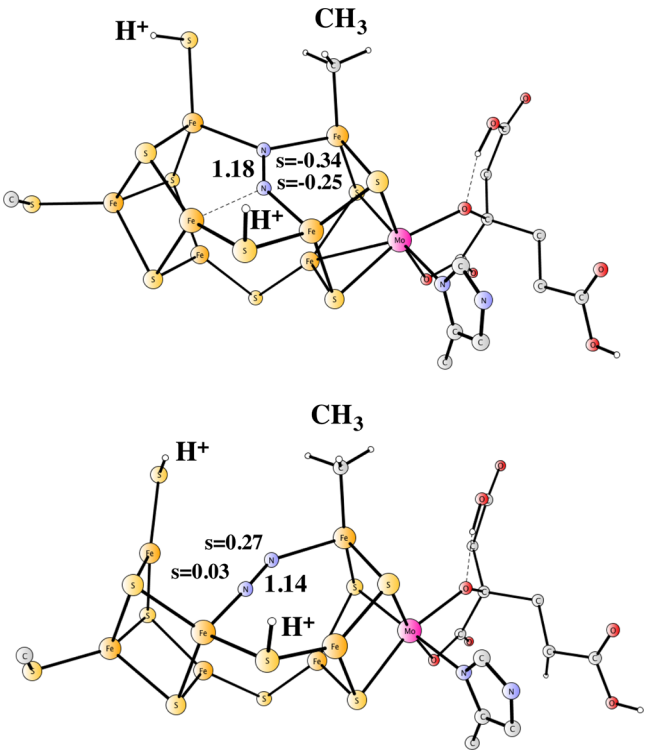

Figure 4. Core structures with N_2 activated. The upper structure is the optimal singlet state; the one below is the optimal triplet state. The electronic structure is $Mo^{3+}4Fe^{2+}3Fe^{1+}$. The spins on the nitrogens are also given, as well as the N−N distance. Surrounding residues and most hydrogen atoms are omitted.

corresponding to a rate of only 0.07 s^{-1}. One reason for this is that with N_2 present the methyl and the nearest SH groups are pushed far away from each other. It is likely that the barrier will continue to be high for the same reason during the entire process from N_2 to ammonia. It should be noted that the formation of methane also has to compete with other processes like the protonation of N_2. How methane formation may be prevented in other cases will be discussed below.

3.2. Alternative Activation. As mentioned in the introduction, a high-resolution structure with a bound CO has recently been obtained.[7] It was surprisingly found that CO replaces the bridging sulfur S2B between Fe2 and Fe6. This result has obviously given rise to speculations that this type of structure where a sulfur has been released and N_2 binds instead of CO is part of the actual activation of the cofactor.[7,20] This possibility has therefore also been investigated in the present study.

The first structure studied was the one suggested by experiments. This structure corresponds to A_2^1 with an unprotonated carbon in the center. It was somewhat surprisingly found that there is a major energy cost to release H_2S to the gas phase (without entropy) by as much as 41.4 kcal/mol. Estimating that the H_2S released binds with 14 kcal/mol to the enzyme (as H_2O to bulk water), this still gives an endergonic release by 27.4 kcal/mol. However, the binding of CO is almost equally exothermic by 39.5 kcal/mol. Subtracting the loss of entropy of 10.7 kcal/mol, the binding free energy becomes 28.8 kcal/mol. This means that the replacement of H_2S by CO is found to be nearly thermoneutral, in agreement with experimental observations of reversability.[7] It is clear that this process cannot occur in two steps but has to be concerted. Most earlier theoretical studies on nitrogenase have used nonhybrid DFT methods (0% exact exchange), so this energy difference was also calculated by reducing the exact exchange to zero. A large exergonicity of 17.8 kcal/mol was then found, in disagreement with experiments. Using the present methods, the enthalpic binding energy of N_2 (instead of CO) at the empty site between Fe2 and Fe6 was found to be very small: only 6.3 kcal/mol. Subtracting the entropy loss of 10.7 kcal/mol upon binding actually makes the binding free energy for N_2 negative by −4.4 kcal/mol. Replacing CO by N_2 is therefore endergonic by 33.2 kcal/mol and cannot occur at this stage.

The possibility that the above process of releasing H_2S could be more favorable after reduction of the cofactor was also investigated. Adding one (e^-, H^+), forming a state corresponding to A_3^1, leads to a cost for removing H_2S of 33.6 kcal/mol keeping a carbon in the center. Again, assuming that H_2S binds with 14 kcal/mol, this leads to an endergonic loss by 19.6 kcal/mol. It should be added at this stage that the preferred state obtained, see above, is not for a carbon but a CH in the center, which is 1.8 kcal/mol lower in energy. The enthalpic binding energy for N_2 after H_2S loss is 10.7 kcal/mol, which is exactly canceled by the loss of entropy of −10.7 kcal/mol. The process of replacing H_2S by N_2 therefore becomes endergonic by 19.6 kcal/mol.

Adding yet another (e^-, H^+), forming a state corresponding to A_4^1, gives a similar picture. Now, removing H_2S is endergonic by 18.3 kcal/mol with an unprotonated carbon in the center, slightly less than the 19.6 kcal/mol discussed above. Again, an unprotonated carbon in the center is not the optimal structure at this stage but is instead one with a CH_2 in the center, which is more favorable by 20.9 kcal/mol. Compared to the CH_2 state, removing H_2S is therefore endergonic by 39.2 kcal/mol. Therefore, adding two (e^-, H^+) to the central carbon is altogether more favorable by 40.5 kcal/mol than to add them to the bridging sulfur and releasing H_2S. Adding N_2 is again endergonic as for the A_3^1 type state.

The present results are therefore not in agreement with a recent study[20] that suggested removing H_2S to bind N_2 in A_2^1. If, in some way, N_2 could replace H_2S in A_2^1, then the energy would be so high that the rest of the ammonia formation could well be downhill, as found in that study. However, both studies agree that a structural change of the cofactor is needed to activate N_2.

3.3. Start of the Catalytic Cycles. In the new scenario, the actual catalytic cycle is only entered after methyl has been formed in the fifth initial reduction step in state A_S^0. The states in the catlytic cycle will here be labeled E-states, with A_S^0 identical to E_3^0. The initial reductions leading to state A_S^0 are therefore suggested not to be part of the catalytic cycle but only to occur once with many catalytic cycles to follow, in which CH_3 is now bound terminally to Fe6. It should be noted that the state entered after the initial four reductions may not be the resting state of the catalytic cycle. To find the resting state of the present mechanism, the full catalytic cycle, including ammonia formation, has to be obtained. The first step after entering the catalytic cycle is that the proton on S3A between Fe4 and Fe5, present in A_S^0, moves into the center of the now empty cavity as a hydride (Figure 5). This step is strongly exergonic by −30.9 kcal/mol. The state before the hydride formation will be termed E_3^0* (the same as the one termed A_S^0 above). The state formed with a hydride in the cavity will be termed E_3^0 and is the ground state at this stage. The large energy difference between these states is highly significant for N_2

DOI: 10.1021/jacs.6b03846
J. Am. Chem. Soc. 2016, 138, 10485−10495

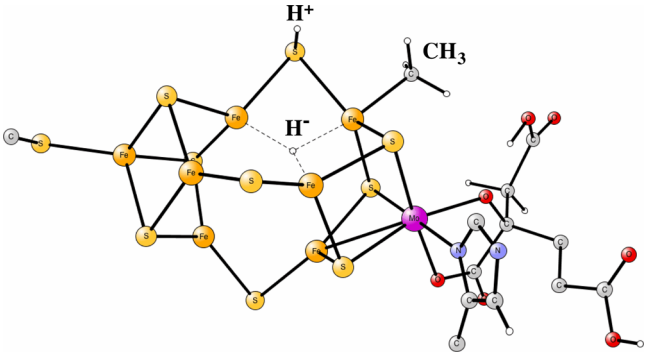

Figure 5. Core structure of the E_3^0 state. The electronic structure is $Mo^{3+}6Fe^{2+}1Fe^{1+}$. Surrounding residues and most hydrogen atoms are omitted.

activation at a later stage. At the end of this step, a proton is accepted by S3A with a pK_a of 10.4 (Table 2), corresponding to

Table 2. Redox and pK_a Values at the Different Stages of the FeMo-Cofactor Reduction[a]

state	protonation site	redox	pK_a	hydrides
E_3^0	H^-			1
E_3^1	S3A		10.4	1
E_4^0		−1.2		1
E_4^1	H^-		9.2	2
E_5^0		−1.1		2
E_5^1			7.0	2

[a]Values start with a new reference state E_3^0 where CH_3 has been formed and moved out of the cavity. There is one proton on sulfur, see the ($+4e^-$, $4H^+$) entry in Table 1. The redox potential of the reference electron donor is −1.6 V. The new reference state is shown in Figure 3.

an exergonic transfer by −4.8 kcal/mol. Alternatively, this ($+e^-$, H^+) transfer step can be described as keeping S3A protonated and the incoming proton going directly into the cavity to form a hydride.

In the second step after entering the actual catalytic cycle, an electron is accepted with a redox potential of −1.2 V, leading to an exergonic transition to state E_4^0 by −10.4 kcal/mol. The next proton taken up will go to a position in the cavity to form a second hydride, with a pK_a of 9.2 in an exergonic transfer by −3.1 kcal/mol (Table 2). After this transfer, there are therefore two hydrides and two protonated sulfurs, S2A and S3B. The state formed is a doublet and is here suggested to be the one that is observed by EPR.[11] From the calculations, an absolute requirement for forming a state with two (or even one) hydrides is therefore, somewhat surprisingly, that the carbon has moved out of the cavity, either as a methyl or as methane. A different conclusion would require that the calculations have an extremely large error, much larger than those seen before using the present methodology.

There is one apparent difference between the present state with two hydrides and the one observed experimentally, and this is that the experimentally observed E_4 state was interpreted as the state that binds N_2, which the present E_4 state does not. To activate N_2, still another electron is needed. The calculated redox potential for this electron is −1.1 V, leading to an exergonic transfer by −11.3 kcal/mol. The activated structure, shown in Figure 6, with the added electron is a singlet state and is therefore not observable by EPR.

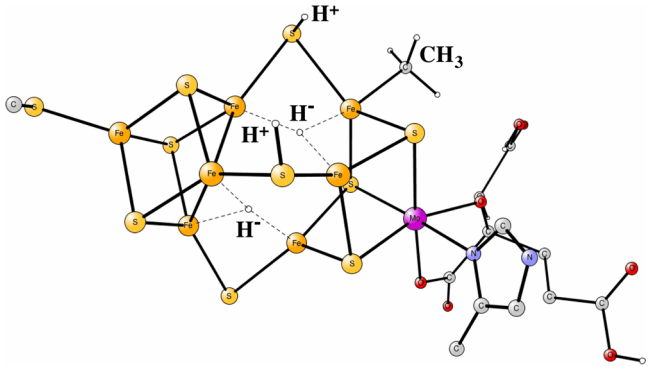

Figure 6. Core structure of the E_5^0 state with two hydrides. The electronic structure is $Mo^{3+}6Fe^{2+}1Fe^{1+}$. Surrounding residues and most hydrogen atoms are omitted.

In the structure with two hydrides, these are bridging between three iron atoms. Experimentally, they were suggested to be bridging only two. However, the discrimination between these types of structures is very hard using just an energy criterion, as done here, since there are several structures with very similar energies. Instead, this could possibly be done using a direct comparison of calculated and experimental spin-spectra. This is beyond the scope of the present study and is therefore postponed to future studies. For the energetics of the catalytic cycle, the question of the preferred binding is unimportant.

3.4. N_2 Activation. In order to activate N_2 after the electron has arrived, several important events were found to occur, very much in line with what has been suggested by spectroscopic studies.[8−15] N_2 does not bind to the structure with two hydrides in Figure 6, so at least one of the hydrides has to leave the cofactor. The only reasonable possibility is that H_2 is formed. The first possibility is a heterolytic mechanism removing one hydride and one proton, previously termed the hp-mechanism. There are four possibilities to do this, and one of them can be ruled out due to a too-long distance between the hydride and the proton. Transition states have been obtained for the other three possibilities, and the one with the lowest energy is shown in Figure 7. The barrier for this

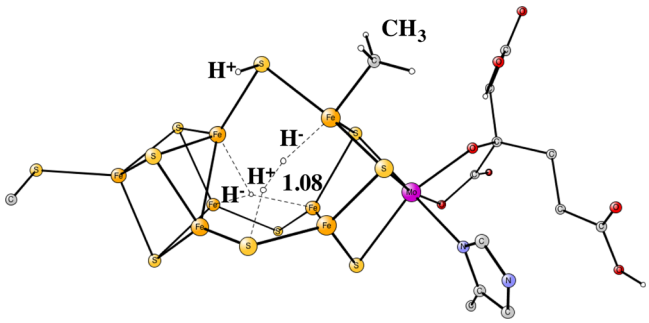

Figure 7. Optimized TS for the heterolytic (hp) mechanism. Surrounding residues and most hydrogen atoms are omitted.

mechanism is 16.7 kcal/mol, which means that it will take 2 s to remove H_2. The product for this mechanism is the structure shown in Figure 5. This is exactly the same structure as already discussed above as the starting point for the catalytic cycle, the E_3^0 state, which does not bind N_2. The two reductions steps following E_3^0 would therefore not have contributed to the

DOI: 10.1021/jacs.6b03846
J. Am. Chem. Soc. 2016, 138, 10485−10495

activation of N_2. The only result would then be just production of H_2.

In order to activate N_2, both hydrides have to be removed, which means a reductive elimination mechanism, previously termed the re mechanism. The optimal transition state obtained is shown in Figure 8. A notable feature of the

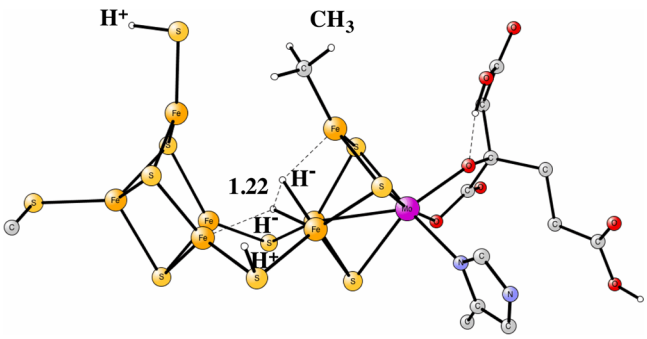

Figure 8. Optimized TS for the reductive elimination (re) mechanism. Surrounding residues and most hydrogen atoms are omitted.

mechanism is that the structure opens up between Fe2 and Fe6, which is required for binding N_2; see below. It is in this context interesting to note that the recent X-ray structure with CO bound to the cofactor has opened up at the same place.[7] The barrier for the re mechanism has to be lower than the one for the hp mechanism in order to activate N_2. The calculations are in agreement with this conclusion and give a barrier of 14.5 kcal/mol, 2.2 kcal/mol lower than the one for the hp mechanism. This means that the wrong path toward H_2 production would be taken once out of 40 cases, which is probably too often compared to experiments. The computed barrier difference is therefore somewhat too small. The TS for the re mechanism has a more open structure than the one for the hp mechanism, so it could have been expected that entropy would favor the re mechanism. However, it did not contribute anything to the energy difference.

Most ealier studies on nitrogenase have used nonhybrid DFT methods (0% exact exchange), so the reaction energies for the re and hp processes were also calculated by reducing exact exchange to zero. The carbon was kept as an atom in the center, also as in most nonhybrid studies. The A_4^1 state was used as suggested by experiments. The result was that the re process led back to the ground state for A_2^1 and did therefore only lead to H_2 production in disagreement with experiments.

After the elimination of the two hydrides, the structure would go to a structurally highly excited state of E_3^0, here termed E_3^0*, which is shown in Figure 9. This state is as much as 30.9 kcal/mol higher in energy than the ground state E_3^0 shown in Figure 5. An interesting point to be noted is that there is another structure of E_3^0* which has opened up between Fe2 and Fe6 that is only a few kcal/mol higher. That structure is more optimal for binding N_2 as shown in Figure 4. The calculated binding energy of H_2 for the E_S^0 state compared to the E_3^0* state is +9.9 kcal/mol. This value contains a large change of dispersion of +16.1 kcal/mol, an effect of entropy of −10.3 kcal/mol for the free H_2 and a change of entropy of the cofactor itself of +2.2 kcal/mol. The change of dispersion is due to a much more compact form of E_S^0 than of E_3^0*.

There is an interesting electronic structure difference between the closed and open form of E_3^0*. In the closed form, the electrons on Fe6 are low-spin-coupled, with a spin-

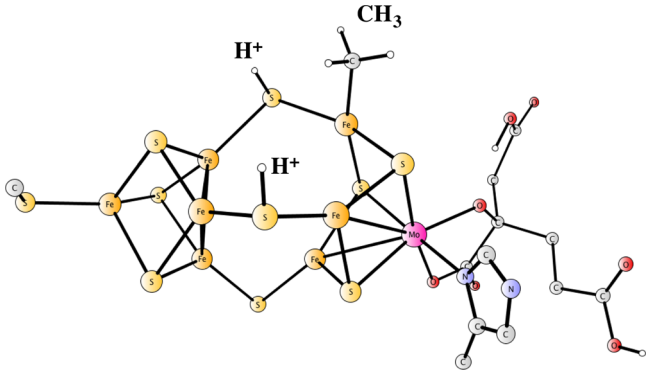

Figure 9. Core structure of the nonoptimal E_3^0* state without a hydride; see also Figure 3 for the identical structure, termed A_S^0. The electronic structure is $Mo^{3+}4Fe^{2+}3Fe^{1+}$. Surrounding residues and most hydrogen atoms are omitted.

population of 2.23. In the open form, they are high-spin-coupled with a spin of 3.64. Also, the closed form is an overall singlet, while the open form is a triplet. These differences make assignment of which structure is lowest rather uncertain since in general low-spin-coupling of the d-electrons is less well described by DFT. This type of low-spin-coupling does not occur for any other structures optimized here.

The opened E_3^0* state can now bind N_2, as already shown in Figure 4. The binding energy for N_2 of −13.8 kcal/mol is just enough to compensate for the loss of entropy of +9.9 kcal/mol compared to the free N_2. The states before and after N_2 binding are therefore quite similar in energy. The possibility that the protons on the sulfurs will move to protonate N_2 has also been investigated, but these types of structures are high in energy indicating that further reductions are needed to reach N_2H_2.

Before the structure in Figure 4 was found, several other structures were investigated, all of them with very poor enthalpic binding to the cofactor. The entropy loss of +9.9 kcal/mol makes them strongly unbound. For example, trying to bind N_2 deep inside the cofactor with bonds to five of the Fe atoms, Fe2−Fe7 (except Fe5), gave a negative binding energy, more than 20 kcal/mol worse than the optimal one.

The agreement between the present results and those deduced from the earlier spectroscopic measurements is quite good. In a very elegant analysis[15,30−32] of the outcome of experiments where D_2 (or T_2) was present in E_4, with and without N_2,[27,44−48] it was concluded that two hydrides are present and that H_2 was removed using the re mechanism and not by the hp mechanism. Furthermore, in a recent study it was found that H_2 release was immediately followed by the activation of N_2. All these key conclusions are confirmed by the present model calculations. Using different pressures of N_2 and H_2, this entire process was found to be reversible, indicating that the states before and after H_2 release and N_2 activation are close in energy.[11] Even though the energy levels for these states are relatively close in the calculations and reachable at room temperature, there appears to be minor discrepancies. For example, the energy level after N_2 binding is 6.1 kcal/mol higher than the one for the E_S^0 state before H_2 release (Figure 10). The reason for this error could be limitations of the models and methods used. As indicated above, an error of the calculated pK_a of His195 has been noted and corrected for in a simple way. Ideally, a larger model should instead be used, which is planned for the future.

DOI: 10.1021/jacs.6b03846
J. Am. Chem. Soc. 2016, 138, 10485−10495

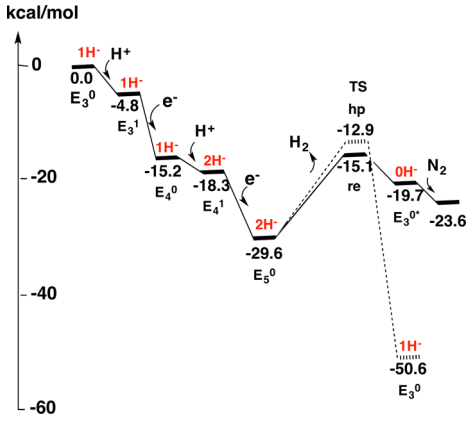

Figure 10. Energy diagram for the start of the catalytic cycle including N_2 binding. The number of hydrides for each state is shown in red.

An interesting effect on the binding of N_2 should be noted. It was found that the binding was entirely lost if a proton reached the unprotonated His195. The binding of N_2 without the proton is +3.9 kcal/mol, going down to −4.0 kcal/mol with the proton on His195, a difference of 7.9 kcal/mol. The reason is that the negative charge is needed in the center of the cofactor for two reasons. The first one is most important and concerns the energy required to open the cluster to bind N_2. From the calculations it can be estimated that it is 5.9 kcal/mol harder to open the cluster with an additional proton on His195. The remaining effect on the difference in binding is 2.0 kcal/mol. Both these effects can be explained by a polarization of the negative charge from the center of the cluster toward the protonated histidine. This could partly have been expected, but the large effect was very surprising. The only solution found to prevent the protonation of His195 was to set its pK_a value to 7. This is the main reason for shifting the pK_a for this group by 5 units. An alternative possibility could have been to assume a high kinetic barrier for the protonation, but this appeared less likely. A rationalization for the pK_a shift is that there is an arginine, Arg277, just outside the model used.

A critical point in the present mechanism, already mentioned above, is that methane formation needs to be hindered. In the activation process of the cofactor (see section 33.1), methane cannot be formed since methyl is only present at the end of this process just before N_2 binds. With N_2 present, or protonated forms of it, the distance is long between methyl and the nearest hydrogen on S2B, leading to high barriers for methane formation. This means that the first critical point is at E_3^1, which is the resting state at that stage. A TS for methane formation has been obtained for a proton from S2B with a barrier of 17.1 kcal/mol, corresponding to a rate of 1 s^{-1}. Even if this is slow, it probably needs to be somewhat slower. A barrier just 2 kcal/mol higher would be enough to prevent methane formation, which is certainly within the uncertainty of the calculations. The next critical point is E_4^1. The same pathway as for E_3^1 with a proton on S2B was found optimal. The computed barrier is 16.4 kcal/mol, which is similar to the case of E_3^1. It is very likely that the enzyme surrounding the cofactor is partly designed to prevent methane formation. His195 is directly hydrogen bonding to S2B, so a tuning of this hydrogen bond strength should be possible to achieve, using the nearby Arg277 and its neighbors.

There have been mnay theoretical studies on the FeMo-cofactor. Most of them have focused on the electronic structure of the cofactor with a central unprotonated atom present. In the earlier studies, the central atom was assumed, or concluded, to be a nitrogen atom. It is now known to be a carbon atom instead, so many of the previous results cannot be directly compared to the present ones. In many of those studies, the charged amino acids in the second shell of the cofactor were furthermore left out. In the present study, two positive arginines and one protonated histidine make the cofactor itself negative by as much as −4. Such a negative cofactor has not been considered before, and the conclusions from these earlier studies about the electronic structure could therefore be questionable. For example, in most previous studies an Mo(IV) was found, which disagrees with both the results obtained here with an Mo(III) and the suggestion by a recent spectroscopic analysis.[25] Furthermore, in the present study it is concluded that the cofactor is quite unreactive with a central unprotonated atom present, making the results of the previous studies even less comparable to the present ones. Direct comparisons to those studies are therefore mostly left out, in order to focus on what is new here.

There is one study by Huniar et al.[21] that is by far most similar to the one here. That study also used calculated energetics to suggest a mechanism for nitrogen fixation. However, there are also major differences compared to the present study, such as the assumption of a nitrogen in the center of the cofactor. Other differences are the use of a nonhybrid functional, lack of dispersion, lack of estimates of entropy effects, no modeling of the surrounding of the cofactor, and so on. Still, many of the results are similar to those obtained here, most strikingly, the full protonation of the central atom and its removal from the cavity before activation of N_2. A central nitrogen atom was assumed in the Huniar study, so the suggestion that the central atom is activated in the catalytic cycle could convincingly be proven wrong by spectroscopy.[22] The suggested mechanism by Huniar et al. has therefore been mostly forgotten and not mentioned in recent reviews even after the identification of the central atom as carbon. In that study N_2 was found to bind inside the cavity with bonds to six Fe atoms. Even though this is similar to the binding to four Fe atoms in the cavity found here, that particular structure was here found to be quite high in energy, more than 20 kcal/mol higher than the optimal one. The main reason for this discrepancy is that a nonhybrid functional was used, which can strongly exaggerate metal bonding. As mentioned above, there are large dispersion effects, but if these had been included, then the discrepancy would have been even larger. The previous study also investigated hydride binding and found structures with the hydrides bound inside the cofactor similar to those found here. However, the hydrides were not considered to play any significant role for the mechanism as they have here and have been shown to have by spectroscopy.[15]

4. CONCLUSIONS

In the present study, the mechanism of nitrogen fixation by nitrogenase has been revisited in light of recent determinations of the presence of a carbon atom in the center of the FeMo cofactor cavity.[5,6] For a long time, the present study did not reach anywhere. No activation of N_2 was found; furthermore, no bound hydrides were found either, even though spectroscopy had convincingly demonstrated the presence of hydrides in the catalytic mechanism. Errors of more than 20 kcal/mol would be required to overturn the present results, and errors of

DOI: 10.1021/jacs.6b03846
J. Am. Chem. Soc. 2016, 138, 10485−10495

this magnitude have never been seen before in similar studies. Thus, other possibilities had to be found.

When other alternatives were investigated, one of the most interesting observations was that the protonation of the central carbon was energetically competitive with the protonation of the sulfides. Furthermore, after the initial reductions of the cofactor and protonation of two bridging sulfides, the only possibility to continue protonation of the cofactor was to also protonate carbon. However, the initial protonation of the carbon was still not enough to activate N_2 or to find bound hydrides. An activation was only found when the carbon was protonated to at least the methyl state and then removed from the cavity. At that stage, the addition of protons led to the formation of two hydrides in the center of the cavity.

Alternative scenarios for activating N_2 would require unusually large errors in the calculations at several situations. First, the computed binding energy for N_2 would in most situations be required to be much larger than the ones computed. Second, the formation energy of hydrides in the case with a central carbon would need to be much larger than obtained here. Third, the computed barriers would need to be much higher for protonation of the central carbon in order to prevent the protonations. All of this would require errors much larger than those seen before in similar studies on redox-active enzymes.[1]

When methyl has been formed and two hydrides have become bound in the E_4^1 state, the activation process of N_2 can start after addition of yet another electron. Binding of N_2 requires the removal of the hydrides from the cavity by a reductive elimination (re) process (Figure 10). A heterolytic removal of a hydride and a proton (hp elimination) only leads back to the previous E_3^0 state which can not activate N_2. The net result of the catalysis would then be just hydrogen and no ammonia formation. After the two hydrides have been removed, a structurally very highly excited E_3^{0*} state is formed, which can bind N_2 with a sufficiently large binding energy to overcome the entropy loss. In this binding, dispersion and entropy effects play a major role.

A critical question in the present mechanism is how methane formation should be prevented. The most obvious cases where methane could be formed have been studied and indeed found to have very large barriers. To know more definitely if they are high enough requires a future study with a large model. In particular, the region around His195 should then be improved.

The present results are in many ways in good agreement with the recent spectroscopic analysis.[15] Through an intricate combination of experiments, it was concluded that a key step in catalysis is the removal of two hydrides by an re mechanism immediately followed by activation of N_2. The good agreement between spectroscopy and calculations has here been taken as a very strong argument for the present mechanism, even though the removal of carbon from the cavity was highly surprising and never suggested before. A remaining question is what purpose the insertion of carbon in the center of the FeMo cofactor plays. A protective, or stabilizing, role for the cofactor appears reasonable. This question cannot be solved by model calculations at present.

■ ASSOCIATED CONTENT

Supporting Information

The Supporting Information is available free of charge on the ACS Publications website at DOI: 10.1021/jacs.6b03846.

Coordinates for the structures in the figures and diagrams (PDF)

■ AUTHOR INFORMATION

Corresponding Author

*per.siegbahn@su.se

Notes

The author declares no competing financial interest.

■ ACKNOWLEDGMENTS

I am grateful to Dr. Rongzhen Liao for several discussions concerning the experimental energetics for ammonia formation by nitrogenase. This work was generously supported by the Knut and Alice Wallenberg Foundation and by grants from the Swedish research council. Computer time was provided by the Swedish National Infrastructure for Computing.

■ REFERENCES

(1) Blomberg, M. R. A.; Borowski, T.; Himo, F.; Liao, R.-Z.; Siegbahn, P. E. M. *Chem. Rev.* **2014**, *114*, 3601−3658.

(2) Siegbahn, P. E. M. *Biochim. Biophys. Acta, Bioenerg.* **2013**, *1827*, 1003−1019.

(3) Kim, J.; Rees, D. C. *Science* **1992**, *257*, 1677−1682.

(4) Einsle, O.; Tezcan, F. A.; Andrade, S. L. A.; Schmid, B.; Yoshida, M.; Howard, J. B.; Rees, D. C. *Science* **2002**, *297*, 1696−1700.

(5) Spatzal, T.; Aksoyoglu, M.; Zhang, L.; Andrade, S. L. A.; Schleicher, E.; Weber, S.; Rees, D. C.; Einsle, O. *Science* **2011**, *334*, 940.

(6) Lancaster, K. M.; Roemelt, M.; Ettenhuber, P.; Hu, Y.; Ribbe, M. W.; Neese, F.; Bergmann, U.; DeBeer, S. *Science* **2011**, *334*, 974−977.

(7) Spatzal, T.; Perez, K. A.; Einsle, O.; Howard, J. B.; Rees, D. C. *Science* **2014**, *345*, 1620−1623.

(8) Igarashi, R. Y.; Laryukhin, M.; Dos Santos, P. C.; Lee, H. I.; Dean, D. R.; Seefeldt, L. C.; Hoffman, B. M. *J. Am. Chem. Soc.* **2005**, *127*, 6231−6241.

(9) Lukoyanov, D.; Barney, B. M.; Dean, D. R.; Seefeldt, L. C.; Hoffman, B. M. *Proc. Natl. Acad. Sci. U. S. A.* **2007**, *104*, 1451−1455.

(10) Barney, B. M.; Lukoyanov, D.; Igarashi, R. Y.; Laryukhin, M.; Yang, T.-C.; Dean, D. R.; Hoffman, B. M.; Seefeldt, L. C. *Biochemistry* **2009**, *48*, 9094−9102.

(11) Lukoyanov, D.; Yang, Z.-Y.; Khadka, N.; Dean, D. R.; Seefeldt, L. C.; Hoffman, B. *J. Am. Chem. Soc.* **2015**, *137*, 3610−3615.

(12) Lukoyanov, D.; Yang, Z.-Y.; Dean, D. R.; Seefeldt, L. C.; Hoffman, B. M. *J. Am. Chem. Soc.* **2010**, *132*, 2526−2527.

(13) Doan, P. E.; Telser, J.; Barney, B. M.; Igarashi, R. Y.; Dean, D. R.; Seefeldt, L. C.; Hoffman, B. M. *J. Am. Chem. Soc.* **2011**, *133*, 17329.

(14) Hoffman, B. M.; Lukoyanov, D.; Dean, D. R.; Seefeldt, L. C. *Acc. Chem. Res.* **2013**, *46*, 587−595.

(15) Hoffman, B. M.; Lukoyanov, D.; Yang, Z. Y.; Dean, D. R.; Seefeldt, L. C. *Chem. Rev.* **2014**, *114*, 4041−4062.

(16) (a) Sandala, G. M.; Noodleman, L. *Methods Mol. Biol.* **2011**, *766*, 293−312. (b) Lovell, T.; Li, J.; Case, D. A.; Noodleman, L. *JBIC, J. Biol. Inorg. Chem.* **2002**, *7*, 735−749. (c) Lovell, T.; Li, J.; Liu, T.; Case, D. A.; Noodleman, L. *J. Am. Chem. Soc.* **2001**, *123*, 12392−12410.

(17) Dance, I. *Inorg. Chem.* **2011**, *50*, 178−192. Dance, I. *Dalton Trans.* **2011**, *40*, 6480−6489. Dance, I. *Dalton Trans.* **2011**, *40*, 5516−5527. Dance, I. *Dalton Trans.* **2010**, *39*, 2972−2983. Dance, I. *Dalton Trans.* **2008**, 5977−5991.

(18) Schimpl, J.; Petrilli, H. M.; Blöchl, P. E. *J. Am. Chem. Soc.* **2003**, *125*, 15772−15778. Kästner, J.; Blöchl, P. E. *J. Am. Chem. Soc.* **2007**, *129*, 2998−3006.

(19) Hinnemann, B.; Nørskov, J. K. *J. Am. Chem. Soc.* **2004**, *126*, 3920−3927.

(20) Varley, J. B.; Wang, Y.; Chan, K.; Studt, F.; Nørskov, J. K. *Phys. Chem. Chem. Phys.* **2015**, *17*, 29541−29547.

DOI: 10.1021/jacs.6b03846
J. Am. Chem. Soc. 2016, 138, 10485−10495

(21) Huniar, U.; Ahlrichs, R.; Coucouvanis, D. *J. Am. Chem. Soc.* **2004**, *126*, 2588−2601.
(22) Lee, H. I.; Benton, P. M. C.; Laryukhin, M.; Igarashi, R. Y.; Dean, D. R.; Seefeldt, L. C.; Hoffman, B. M. *J. Am. Chem. Soc.* **2003**, *125*, 5604.
(23) Harris, T. V.; Szilagyi, R. K. *Inorg. Chem.* **2011**, *50*, 4811−4824.
(24) Yan, L.; Pelmenschikov, V.; Dapper, C. H.; Scott, A. D.; Newton, W. E.; Cramer, S. P. *Chem. - Eur. J.* **2012**, *18*, 16349−16357.
(25) Bjornsson, R.; Lima, F. A.; Spatzal, T.; Weyhermueller, T.; Glatzel, P.; Bill, E.; Einsle, O.; Neese, F.; DeBeer, S. *Chem. Sci.* **2014**, *5*, 3096−3103.
(26) *CRC Handbook of Chemistry and Physics*, 85th ed.; Lide, D. R., Ed.; CRC Press: Boca Raton, FL, 2004.
(27) Burgess, B. K.; Lowe, D. J. *Chem. Rev.* **1996**, *96*, 2983−3011.
(28) Rees, D. C. *Annu. Rev. Biochem.* **2002**, *71*, 221.
(29) Veech, R. L.; Lawson, J. W. R.; Cornell, N. W.; Krebs, H. A. *J. Biol. Chem.* **1979**, *254*, 6538−6547. Bergman, C.; Kashiwaya, Y.; Veech, R. L. *J. Phys. Chem. B* **2010**, *114*, 16137−16146.
(30) Shaw, S.; Lukoyanov, D.; Danyal, K.; Dean, D. R.; Hoffman, B. M.; Seefeldt, L. C. *J. Am. Chem. Soc.* **2014**, *136*, 12776−12783.
(31) Yang, Z.-Y.; Khadka, N.; Lukoyanov, D.; Hoffman, B. M.; Dean, D. R.; Seefeldt, L. C. *Proc. Natl. Acad. Sci. U. S. A.* **2013**, *110*, 16327−16332.
(32) Lukoyanov, D.; Yang, Z. Y.; Duval, S.; Danyal, K.; Dean, D. R.; Seefeldt, L. C.; Hoffman, B. M. *Inorg. Chem.* **2014**, *53*, 3688−3693.
(33) Becke, A. D. *J. Chem. Phys.* **1993**, *98*, 5648−5652.
(34) Reiher, M.; Salomon, O.; Hess, B. A. *Theor. Chem. Acc.* **2001**, *107*, 48−55.
(35) Siegbahn, P. E. M. *JBIC, J. Biol. Inorg. Chem.* **2006**, *11*, 695−701.
(36) Siegbahn, P. E. M.; Himo, F. *JBIC, J. Biol. Inorg. Chem.* **2009**, *14*, 643−651.
(37) Siegbahn, P. E. M.; Himo, F. *Comput. Mol. Sci.* **2011**, *1*, 323−336.
(38) Grimme, S. *J. Chem. Phys.* **2006**, *124*, 034108. Schwabe, T.; Grimme, S. *Phys. Chem. Chem. Phys.* **2007**, *9*, 3397−3406.
(39) *Jaguar 5.5,*; Schrödinger, L.L.C.: Portland, OR, 2003.
(40) Frisch, M. J.; Trucks, G. W.; Schlegel, H. B.; Scuseria, G. E.; Robb, M. A.; Cheeseman, J. R.; Scalmani, G.; Barone, V.; Mennucci, B.; Petersson, G. A.; Nakatsuji, H.; Caricato, M.; Li, X.; Hratchian, H. P.; Izmaylov, A. F.; Bloino, J.; Zheng, G.; Sonnenberg, J. L.; Hada, M.; Ehara, M.; Toyota, K.; Fukuda, R.; Hasegawa, J.; Ishida, M.; Nakajima, T.; Honda, Y.; Kitao, O.; Nakai, H.; Vreven, T.; Montgomery, J. A., Jr.; Peralta, J. E.; Ogliaro, F.; Bearpark, M.; Heyd, J. J.; Brothers, E.; Kudin, K. N.; Staroverov, V. N.; Kobayashi, R.; Normand, J.; Raghavachari, K.; Rendell, A.; Burant, J. C.; Iyengar, S. S.; Tomasi, J.; Cossi, M.; Rega, N.; Millam, J. M.; Klene, M.; Knox, J. E.; Cross, J. B.; Bakken, V.; Adamo, C.; Jaramillo, J.; Gomperts, R.; Stratmann, R. E.; Yazyev, O.; Austin, A. J.; Cammi, R.; Pomelli, C.; Ochterski, J. W.; Martin, R. L.; Morokuma, K.; Zakrzewski, V. G.; Voth, G. A.; Salvador, P.; Dannenberg, J. J.; Dapprich, S.; Daniels, A. D.; Farkas, O.; Foresman, J. B.; Ortiz, J. V.; Cioslowski, J.; Fox, D. J. *Gaussian 09*, revision E.01; Gaussian, Inc.: Wallingford, CT, 2009.
(41) Siegbahn, P. E. M.; Blomberg, M. R. A. *Chem. Rev.* **2010**, *110*, 7040−7061.
(42) Siegbahn, P. E. M.; Tye, J. W.; Hall, M. B. *Chem. Rev.* **2007**, *107*, 4414−4435.
(43) Hu, Y.; Ribbe, M. W. *JBIC, J. Biol. Inorg. Chem.* **2014**, *19*, 731−736.
(44) Burgess, B. K.; Wherland, S.; Newton, W. E.; Stiefel, E. I. *Biochemistry* **1981**, *20*, 5140.
(45) Li, J.-L.; Burris, R. H. *Biochemistry* **1983**, *22*, 4472.
(46) Jensen, B. B.; Burris, R. H. *Biochemistry* **1985**, *24*, 1141.
(47) Hoch, G. E.; Schneider, K. C.; Burris, R. H. *Biochim. Biophys. Acta* **1960**, *37*, 273.
(48) Jackson, E. K.; Parshall, G. W.; Hardy, R. W. F. *J. Biol. Chem.* **1968**, *243*, 4952.

DOI: 10.1021/jacs.6b03846
J. Am. Chem. Soc. 2016, 138, 10485−10495